The cellular mammalian clock regulates *Staphylococcus aureus* invasion in epithelial cells

Pooja Agarwal[1], Giridhar Chandrasekharan[1], Sreshtha Nayek[1], Jaspreet Grewal[1], Robert Dallmann[1,2,*] and Meera Unnikrishnan[1,*]

[1] Division of Biomedical Sciences, Warwick Medical School, University of Warwick, Coventry, UK

[2] Zeeman Institute for Systems Biology & Infectious Disease Epidemiology Research (SBIDER), University of Warwick, Coventry, UK

* Corresponding authors

Addresses for correspondence:

r.dallmann@warwick.ac.uk and m.unnikrishnan@warwick.ac.uk

Abstract

An endogenous biological clock, the circadian clock, coordinates life with the 24-hour day/night environmental cycle. In mammals, a central pacemaker in the suprachiasmatic nucleus of the hypothalamus coordinates timing between peripheral clocks and with the environment and, for example, modulates immune responses to infections. However, its role in controlling bacterial infections at a cellular level is not understood. Here, we investigate the role of the host cellular clock during infection by a highly drug-resistant human pathogen, *Staphylococcus aureus.* Our findings revealed that *S. aureus* invasion into epithelial cells was dependent on the host circadian phase. Interestingly, cells deficient in BMAL1*,* a transcriptional activator and an essential clock protein, demonstrated increased bacterial uptake compared to parental A549 cells. The *BMAL1*-knockdown (KD) cells showed significant induction of GP340, a receptor of the *S. aureus* adhesin, SraP. An *S. aureus sraP* mutant did not exhibit rhythmic uptake into A549 cells or an increased uptake into *BMAL1*-KD compared to parental A549 cells. Of note, other bacterial adhesin mutants showed rhythmic and higher uptake in *BMAL1*-KD cells. Hence, we report that *S. aureus* epithelial cell invasion is clock-modulated and mediated through the *S. aureus* SraP-GP340 pathway, suggesting potential for host clock-directed therapy against this pathogen.

37 **Introduction**

38 Circadian rhythms are intrinsic, about 24-hour cycles that govern a wide array of
39 physiological processes in most living organisms, ranging from bacteria to humans[1,2].
40 These rhythms are regulated by a cell autonomous internal time-keeping system
41 known as the circadian clock, which allows organisms to anticipate and adapt to daily
42 environmental changes, synchronize metabolic functions, and maintain overall
43 homeostasis[3].

44 In mammals, a central clock in the hypothalamic suprachiasmatic nucleus (SCN)
45 coordinates rhythms in all other organ, tissue and cellular clocks relative to the
46 environmental light/dark cycles. The molecular basis of circadian rhythms involves
47 coupled transcriptional-translational feedback loops consisting of more than a dozen
48 core clock genes[1], including the central positive and negative arm transcription factors
49 BMAL1, CLOCK and PERIODs, CRYPOTCHROMEs, respectively. These genes
50 interact to produce proteins that oscillate in abundance over an approximate 24-hour
51 cycle, ultimately regulating downstream processes involved in metabolism, immunity,
52 inflammation and various physiological responses[3].

53 Recent research has underscored the significant influence of the circadian clock on
54 immune regulation and host-pathogen interactions[4,5]. The synchronization between
55 the circadian system and immune responses ensures that the body can efficiently
56 combat pathogens at optimal times of the day[6]. For example, studies have shown that
57 immune cells exhibit diurnal variations in activity, with certain populations peaking at
58 specific times, thereby enhancing the body's ability to respond to infections[7].
59 Disruptions to circadian regulation, whether due to genetic, environmental, or
60 behavioural factors, can impair these defences, leading to increased susceptibility to
61 infections and altered pathogen behaviour[8,9]. Additionally, dysregulation of the host
62 circadian clock has been linked with increased susceptibility to bacterial infection[10].

63 *Staphylococcus aureus*, a Gram-positive bacterium, is a highly drug-resistant
64 opportunistic human pathogen responsible for a wide range of infections, from minor
65 skin conditions to life-threatening diseases such as pneumonia, endocarditis, and
66 sepsis[11,12]. *S aureus* is a facultative intracellular pathogen, which invades a range of
67 mammalian cells, which offer a niche for replication, persistence and resistance to
68 antimicrobials[13-16]. Recent findings suggest that disruption of circadian regulation can

impair immune responses towards *S. aureus* infection[17]. However, at a cellular level, the molecular mechanisms underlying the role of the host clock in *S. aureus* infection remain unclear. Identifying host pathways involved may lead to the development of chronotherapeutic approaches that optimize timing for interventions against *S. aureus* infections.

In this study, we explore the role of the host circadian clock in modulating *S. aureus* infection of epithelial cells in an *in vitro* infection model. We demonstrate that *S. aureus* invasion is dependent on the mammalian circadian phases and that specific bacterial adhesins may control rhythmic invasion through interactions with clock-regulated host proteins. This study implicates potential molecular targets that could inform new strategies against *S. aureus* infection.

80 **Methods and Materials**

81 **Bacterial strains, plasmids, and bacterial culture conditions**

82 *Staphylococcus aureus* strains, *S. aureus* JE2 wild-type (WT) (BEI Resources),
83 including *S. aureus* reporter strains (containing pMV158-mCherry or pMV158-GFP),
84 *S. aureus*::mCherry (pOS1), *S. aureus*::GFP (pMV158), were cultured in tryptic soy
85 broth (TSB, Merck) medium at 37°C with shaking, in the presence or absence of
86 5 µg/mL tetracycline, as appropriate.

87 Transposon mutants from the Nebraska transposon mutant
88 library (https://ntml.unmc.edu) were obtained from BEI Resources for key adhesion
89 factors, including FnbA (fibronectin-binding protein A) NR-46609, FnbB (fibronectin-
90 binding protein B) NR-47271, and SraP (serine-rich adhesin for platelets) NR-46576.
91 These mutants were cultured in Tryptic Soy broth (TSB) containing 5 µg/mL
92 erythromycin as per instructions.
93 For infection experiments, bacterial cultures were initiated from frozen stocks one day
94 before the assay and overnight cultures were prepared. On the day of the experiment,
95 log-phase cultures were initiated by diluting the overnight cultures into fresh TSB
96 medium. Bacteria were grown in a shaker at 37°C to an optical density at 600 nm
97 (OD_{600}) of 1.0, which is exponential growth phase for *S. aureus* JE2.

98 **Mammalian cell culture and circadian synchronization**

99 Human lung epithelial adenocarcinoma A549 cells wild type (ATCC CCL-185) with or
100 without sh*BMAL1* knockdown were cultured in high glucose DMEM supplemented with
101 GlutaMAX (11584516, Gibco), 1% Penicillin/Streptomycin (P4458, Sigma-Aldrich) and
102 dialysed 10% fetal bovine serum (FBS, 26400044, Gibco). Cells were maintained in a
103 humidified atmosphere at 37°C with 5% CO_2. To evaluate *Staphylococcus aureus*
104 invasion, mammalian cells were seeded in 24-well plates (662892, Greiner) or 4-
105 chamber (177399, Nunc Lab-Tek) slides at a density of 3×10^5 cells per well and
106 incubated for 24 hours prior to infection.

107 For circadian synchronization experiments, cells were seeded at a density of
108 2×10^5 cells per well and allowed to adhere for 24 hours. Synchronization was
109 achieved using forskolin (FSK, 10 µM, S2449, Selleck Chemicals), a potent cyclic AMP
110 (cAMP) activator known to reset the circadian clock of all cells in the culture vessel to

111 a common phase[18,19]. Using this widely employed method, cellular clocks were reset
112 6, 12, 18, or 24 h before infection with *S. aureus* to assess circadian phase difference
113 of bacterial invasion (Figure 1A). The time from FSK treatment is used as a phase-
114 marker throughout.

115 For microscopy-based assessments, cells were seeded either in imaging 24-well
116 plates or on 4-chamber slides to facilitate imaging of *S. aureus* interactions with
117 epithelial cells.

118 **Generation of transgenic A549 cell lines**

119 *BMAL1* knockdown cells were generated by lentiviral transgenesis following a
120 published strategy[20]. In short, lentiviral particles were generated by transfection of
121 HEK293FT cells (R70007, Invitrogen) with a third generation lenti-viral backbone
122 pGIPZ for *shBMAL1* packaging and capsid plasmids (pCMVR8.74 and pMD2.G,
123 Addgene) using TransIT-LT reagent (Mirrus Bio) as described[21]. Supernatant
124 containing viral particles was sterile filtered and frozen at -80ºC until use. For lentiviral
125 transduction, viral supernatant with 8 µg/mL polybrene (TR-1003G, Sigma-Aldrich)
126 was added onto 60% confluent A549 cells, and incubated at 37ºC for 6 h, after which
127 cells were washed and incubated for 3 days in standard media. Afterwards, media was
128 supplemented with 10 µg/ml puromycin to select infected cells. Co-expressed eGFP
129 was assessed as further confirmation that cells had integrated the *shBMAL1* construct.

130 **Invasion and survival assays**

131 To evaluate the invasion of A549 cells, *S. aureus* cultured to OD_{600} of 1.0 (logarithmic
132 growth phase) were harvested by centrifugation at 5000 xg for 10 minutes and washed
133 twice with phosphate-buffered saline (PBS). The bacterial pellet was resuspended in
134 PBS and the required volume of this culture was added to the cell culture medium to
135 prepare the inoculum at 3–6 x 10^6 CFU/ml. This inoculum was added to epithelial cells
136 (1 ml/well), for 1 h to achieve a multiplicity of infection (MOI) of 10:1. Inoculum bacterial
137 counts and MOI's were confirmed by bacterial colony counts and epithelial cell counts
138 for each experiment. Following the infection period, extracellular bacteria were
139 removed by incubating cells in culture medium containing gentamicin (50 µg/mL) and
140 lysostaphin (20 µg/mL) for 30 minutes. The cells were then washed three times with
141 PBS and lysed with cold water to release intracellular bacteria. To enumerate colony
142 forming units (CFU), cell lysates were serially diluted and plated onto tryptic soy agar

143 (TSA; Sigma). To monitor the intracellular growth kinetics of bacteria using
144 microscopy, infected cells were incubated with 2 µg/mL lysostaphin. Imaging was
145 performed using either a BioTek Cytation 5 Multimode Reader (Agilent) or a confocal
146 microscope (Olympus FV3000).

147 Analysis of rhythmic patterns for synchronised cells infected with *S. aureus* was
148 conducted on bacterial CFU or the fold-changes of internalised bacterial CFU/ml
149 (bacterial invasion) relative to unsynchronised cells. A COSINOR model was used as
150 previously described [22], using the equation Y=(Mesor+Amplitude*cos(((2*pi)*(X-
151 Acrophase))/Period)) with constraining Period to over 20 h. The linear model was Y=
152 YIntercept + X*Slope with no further constraint. Data was fit to COSINOR and linear
153 models and an extra sum-of-squares F-test was run at $P < 0.01$ with the linear model
154 as null hypothesis.

155 **RNA-Seq and data analysis**

156 To harvest RNA, parental and *shBMAL1* A549 cells were seeded and synchronised
157 by FSK as described above. RNA was extracted at the indicated times post
158 synchronisation using the RNeasy Plus kit (74134, Qiagen). Briefly, the cells were
159 washed thrice in PBS and lysed in the RLT buffer from the kit. Genomic DNA was
160 removed from the lysate using a gDNA eliminator spin column from the kit. 1 volume
161 of 70% ethanol was added to the flowthrough and loaded on a RNeasy spin column.
162 The column was centrifuged at 8000 xg for 30 s. This was followed by subsequent
163 washes with RW1 and RPE buffer. Excess ethanol from the column was removed by
164 spinning the column at 13000 xg for 1 min. Twenty ml RNase free buffer was added
165 to the column and spun at 8000 xg for 1 min. RNA was quantified using the Qubit
166 assay. The RNA samples (30 ng/µl) were sent to Novogene for library preparation
167 after poly(A) enrichment and subsequently sequenced using a pair-ended 150 bp kit
168 on an Illumina NovaSeq. Sequencing depth was at least 15 million reads per sample.
169 Gene count tables were generated using Kallisto on the BioJupies platform[23]. All
170 further analysis was conducted using iDEP 2.0[24]. The DESeq2 algorithm was used for
171 differential gene expression analysis with FDR cutoff of 0.01. For gene normalisation
172 variance stabilising transformation (VST) was used for data in PCA, heatmap. Single
173 gene expression levels are reported as log2CPM+1 values transformed with
174 EdgeR[25,26]. Parametric Gene Set Enrichment Analysis (PGSEA) of KEGG pathways

175 was used for pathway analysis with FDR cutoff of 0.0001[27]. RNA-Seq data are
176 available at the ELIXIR database ArrayExpress under accession number E-MTAB-
177 15036.

178 **Western blotting**

179 To prepare cell lysates, synchronized and non-synchronised cells were lysed using
180 RIPA buffer. Samples were separated on a 4-12% SDS-PAGE gels (Mini-PROTEAN
181 TGX) and then transferred onto a nitrocellulose membrane (Bio-Rad) using wet
182 transfer. The membrane was blocked for 1 hour with 5% non-fat milk and then
183 incubated overnight at 4°C with 1 mg/ml anti-BMAL1 mAb (Abcam, 93806), diluted
184 1:2000. Membranes were washed three times with Tris buffered saline with 0,1%
185 Tween-20 (TBS-T) and incubated with a 1:2000-diluted HRP-conjugated secondary
186 goat anti-mouse antibody (Abcam, 205718) for 1 hour at room temperature (RT). After
187 washing three times with TBS-T, the signal was detected using a Pierce ECL Western
188 Blot Substrate (Thermo Scientific, 10005943) according to the manufacturer's
189 instructions.

190 The blot was then stripped using stripping buffer, washed with TBS-T, blocked again
191 for 1 hour with TBS containing 5% non-fat milk, and incubated overnight at 4°C with 1
192 mg/ml anti-Actin mAb (Sigma A5316), diluted 1:2000. The next day, membranes were
193 washed three times with TBS-T and incubated with a 1:2000-diluted HRP-conjugated
194 secondary goat anti-mouse antibody (Abcam, ab8227) for 1 h at RT followed by
195 detection with ECL substrate as above.

196 **Flow cytometry**

197 We used flow cytometry to quantify GP340 protein expression in parental A549 cells
198 from four 6-hourly samples taken at 6, 12, 18 and 24 h after FSK synchronisation as
199 described above, and from unsynchronised cells to compare A549 parental with
200 *shBMAL1* cells. For this, live cells were trypsinized, >95% viability confirmed, washed
201 in PBS and density adjusted to 1×10^6 cells/ml. After blocking of cells with 1% BSA in
202 PBS for 30 min, they were pelleted and stained with anti-GP340 rabbit antibody (1:500,
203 Thermofisher, PA5-115313) in 1% BSA in PBS and incubated at 4°C for 1 h in dark.
204 Before and after staining with secondary anti-rabbit IgG Alexa Fluor 647 conjugated
205 antibody (1:1000, Cell Signalling, 4414) for 1 h in the dark, cells were washed three
206 times in PBS, resuspended, and 30,000 events were recorded in triplicate in a flow

207 cytometer (BD Biosciences LSRFortessa) for analysis. The round-the-clock
208 experiments were performed on two independent occasions in triplicate and results
209 were normalised to the average GP340+ per sample and then pooled for COSINOR
210 analysis as described above.

211 **Microscopy and image analysis**

212 For bacterial visualization via confocal microscopy, cells were fixed with 4%
213 paraformaldehyde (PFA) for 1 hour, followed by three washes with PBS. Actin was
214 stained with Phalloidin 650 in the dark for 1 h. After staining, cells were washed three
215 times with PBS, air-dried, and mounted using a mounting medium containing DAPI for
216 nuclear staining. Stained samples were observed using an Olympus FV3000 Confocal
217 Laser Scanning Microscope. Images were analysed with ImageJ using Fiji[28]. The
218 imaging parameters are included in supplementary materials. Image analysis for data
219 recorded on the Cytation 5 was conducted using the BioTek Gen5 software. For time-
220 lapse microscopy, for each sample, a region of interest (ROI) was identified and
221 fluorescence tracked over a 24 h period.

222

223 **Results**

224 ***S. aureus* invasion of human lung epithelial cells is dependent on circadian**
225 **phase**

226 To investigate the role of the circadian clock in the invasion of *S. aureus*, A549 human
227 lung adenocarcinoma cells were synchronized using forskolin (FSK). A549 cells are
228 well known to contain a functional clock[29] and FSK is a well-known cAMP inducer
229 commonly employed for cellular clock synchronization[19]. We confirmed circadian
230 oscillations in the A549 cells synchronised with FSK by creating and recording from
231 an A549;*Per2-luc* reporter cell line (Figure S2A).

232 Epithelial cells were synchronised by forskolin in 6-hourly intervals over a 24-h period
233 and subsequently infected with *S. aureus* for 1 h. In addition, unsynchronised A549
234 cells were infected (Figure 1A). Notably, compared to unsynchronised cells, a higher
235 number of intracellular bacteria was observed in synchronised cells after 12 h before
236 infection, as measured by colony forming units (CFU), whereas a significantly lower
237 uptake was detected in cells synchronised 24 h before infection. These findings
238 suggest that the phase of the cellular circadian clock modulates the uptake of
239 *S. aureus* (Figure 1B). Non-linear curve fitting using COSINOR analysis suggested a
240 significant rhythmicity with and approximately 3-fold change in colony-forming units
241 (CFU) between the 12 h and 24 h samples (sum-of-squares F-test, $P = 0.0001$, Figure
242 1C).

243 To verify this result and visualize intracellular bacterial foci, confocal microscopy was
244 performed on fixed samples infected at different circadian phases as above. We found
245 a higher number of intracellular bacteria within cells synchronised 12 h before infection
246 compared to those 24 h before. Quantification of these samples showed on average
247 of ~3 bacteria per mammalian cell 12 h after FSK synchronisation, while this
248 decreases at 24 h post FSK to 1.5 bacteria per cell (Figure 1E), reinforcing the notion
249 that the host's circadian clock may play a modulating role in bacterial uptake with an
250 amplitude of 2-3-fold.

251 We further monitored the intracellular growth kinetics of *S. aureus* in the presence of
252 5 µg/ml lysostaphin, which kills extracellular bacteria (Figure S1A) for 12 h after

253 infection of A549 cells using fluorescence time-lapse imaging. As above, synchronised
254 A549 cells were infected at four distinct circadian phases. Consistent with results for
255 invasion, our data showed a steeper increase in bacterial foci in the earlier time (6 h
256 and 12 h) and a longer time to reach peak intracellular bacterial load (Figure S1B).
257 Together our findings highlight a potential role for the circadian clock in modulating
258 mammalian host cell factors for *S. aureus* cell invasion.
259

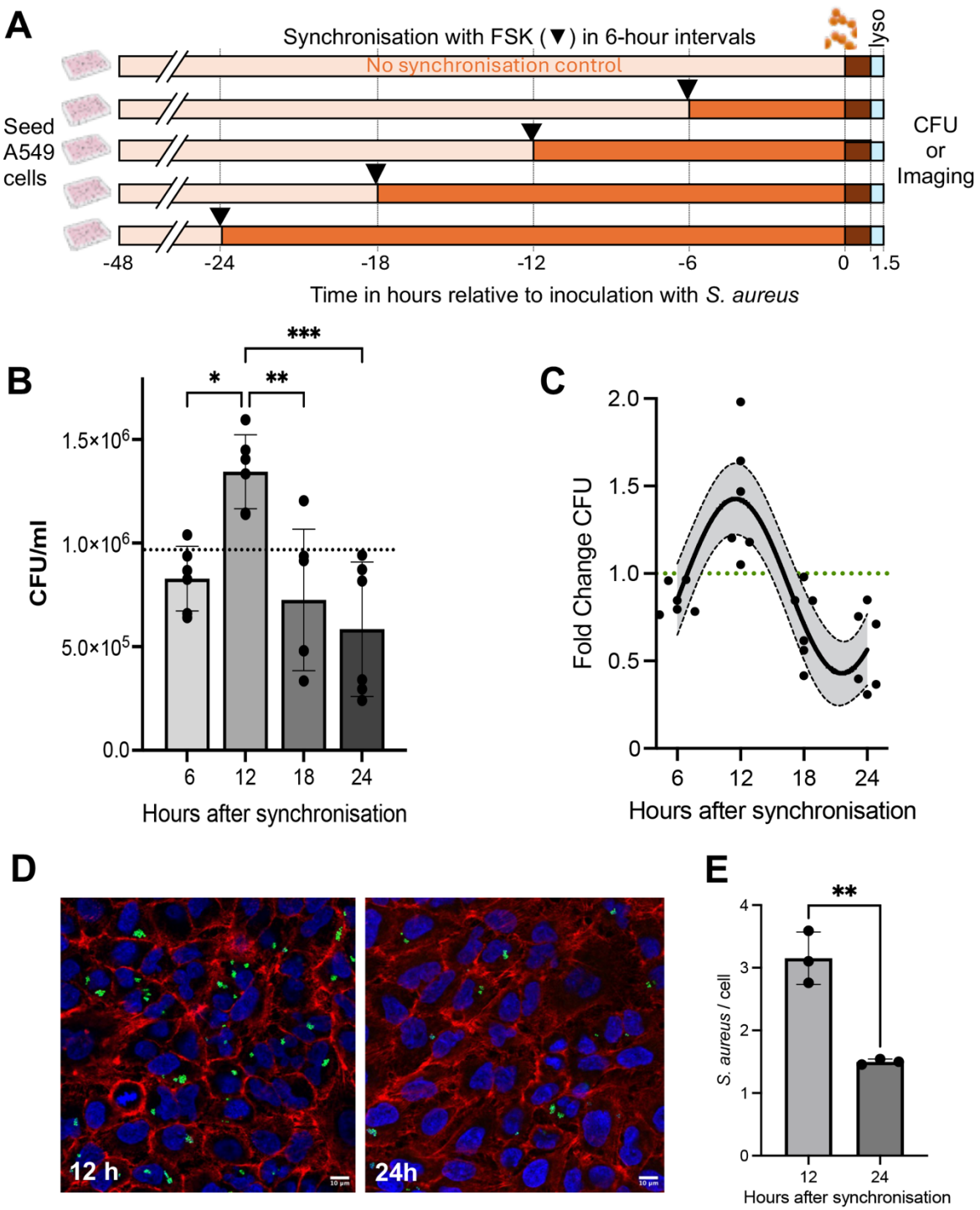

Figure 1. *S. aureus* invasion is modulated by epithelial cell circadian phase. (A) Schematic diagram showing experimental design. A549 cells were synchronized with forskolin (FSK) 24, 18, 12 and 6 h before infection with bacteria at an MOI of 10:1. FSK synchronized or unsynchronized cells were infected with wildtype USA300JE2 *S. aureus* for 1 h, and extracellular bacteria were removed by gentamicin/lysostaphin treatment. (**B**) Intracellular bacterial numbers determined by colony counts (CFU) from

267 different times after synchronization (green dashed line shows value for mean
268 unsynchronized cells), mean ± standard deviation (SD), * P = 0.014, ** P = 0.0031
269 and *** P = 0.004 by one way ANOVA with a Tukey's multiple comparisons test, N =
270 6. (**C**) Data from B plotted as fold-change in CFU compared to an unsynchronized
271 control showing COSINOR best fit with 95% confidence interval. (**D**) Confocal images
272 of epithelial cells, synchronized by FSK for 24 h and 12 h, green - foci of intracellular
273 *S. aureus*-GFP, Red - actin stained by Phalloidin Alexa fluor 647, Blue - nuclei stained
274 by DAPI. Scale bar = 10 μm. A single Z-section is shown (**E**) Bacteria (green) and cell
275 nuclei (blue) were counted manually and the relative number of bacteria to A549 cells
276 was calculated from 3 independent experiments, mean ± SD, P = 0.003, unpaired t-
277 test.

278

279 **Rhythmic *S. aureus* invasion is lost in clock-disrupted human epithelial cells**
280 To investigate if the observed changes are driven by the canonical circadian clock, we
281 generated clock-disrupted A549 cells by targeting the transcription factor BMAL1, an
282 essential core circadian clock gene[1,30]. We generated *BMAL1* knockdown (*shBMAL1*)
283 A549 cells using a lentiviral transduction system. Successfully transfected cells were
284 selected based on puromycin resistance conferred by the presence of the knockdown-
285 construct and confirmed by eGFP expression (Figure S2B). Downregulation of BMAL1
286 protein expression was confirmed via western blot analysis (Figure 2A). Quantitative
287 densitometric analysis of the blots revealed a 50% reduction in BMAL1 protein levels
288 in knockdown cells compared to parental A549 cells (Figure 2A). Gene expression
289 profiling with RNA-Seq also confirmed downregulation of *BMAL1* mRNA and pathway
290 analysis suggested a disruption of the KEGG pathway for "circadian rhythm" (Figure
291 S2C).

292 We then tested the clock disrupted *shBMAL1* A549 cells in the infection assay with
293 *S. aureus* as described above. Unlike parental cells, which again exhibited a circadian
294 phase-dependent rhythm of bacterial invasion, a temporal invasion pattern was
295 abolished in *shBMAL1* A549 cells (Figure 2C,D). Non-linear COSINOR fit the data
296 statistically worse than a linear model for *shBMAL1* cells (sum-of-squares F-test,
297 P = 0.0151; Figure 2C,D). This observation strongly suggests the circadian clock, for
298 which *BMAL1* is a critical regulator, is necessary for *S. aureus* invasion rhythms in
299 A549 cells.

300 Interestingly, our data in *shBMAL1* A549 cells suggests an increase in *S. aureus*
301 invasion irrespective of time after synchronization. Quantitative CFU analysis showed
302 that the uptake in knockdown cells was approximately 1.7-fold higher than in parental
303 A549 cells (Figure 2E). Furthermore, intracellular bacterial survival after 24 hours was
304 also higher for *shBMAL1* cells (Figure 2F). To visualize intracellular bacteria, we
305 performed confocal microscopy on fixed mammalian cells. Consistent with the CFU
306 data, microscopy images confirmed a greater number of intracellular bacteria in
307 sh*BMAL1* cells compared to the parental line (Figure 2G,H). The significantly higher
308 bacterial burden in *BMAL1* knockdown cells highlights its role as a regulator of host-
309 pathogen interactions, potentially through pathways that influence cellular processes
310 such as bacterial recognition, adhesion, or uptake.

311

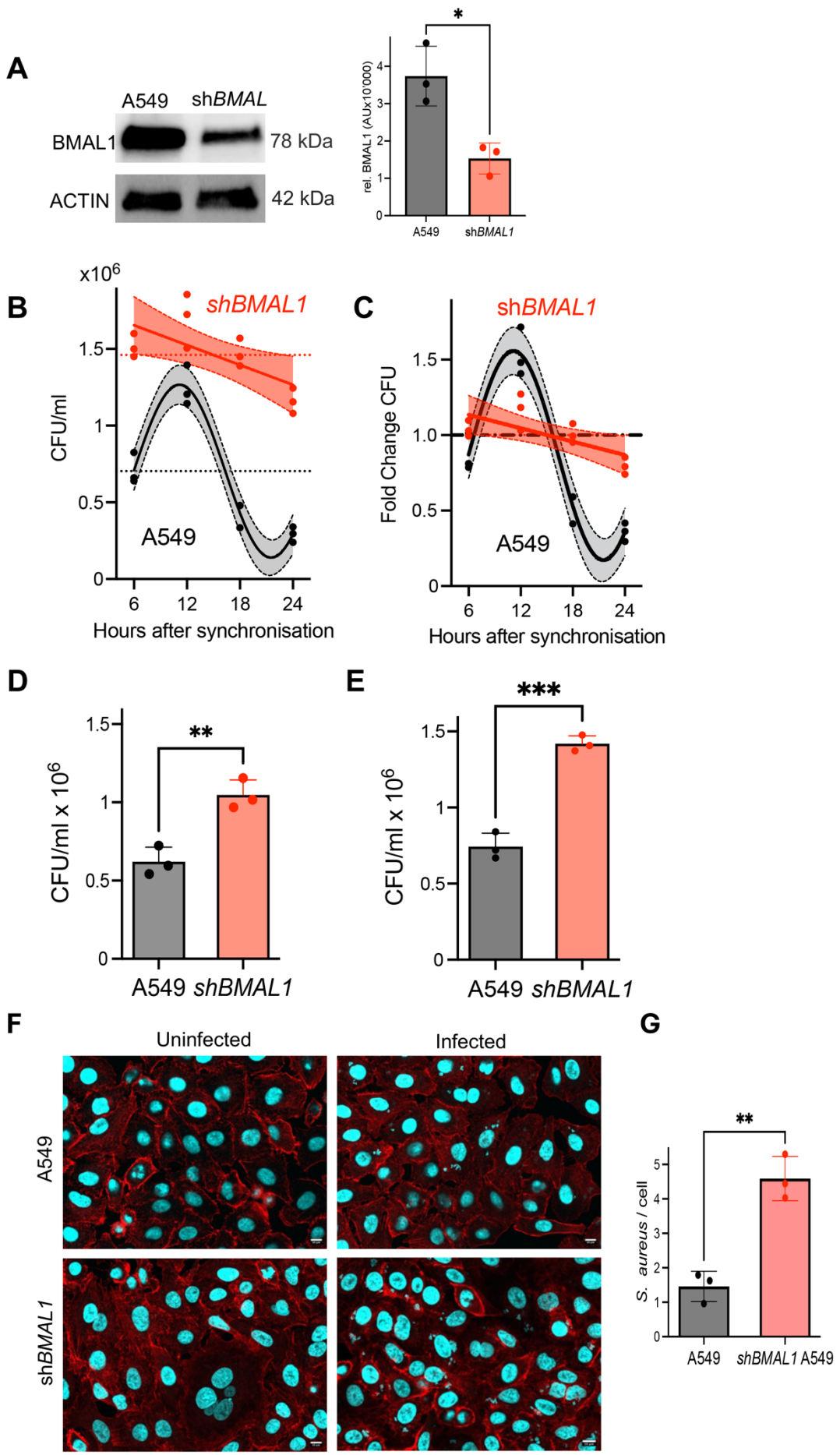
A
A549
shBMAL
BMAL1
78 kDa
ACTIN
42 kDa
rel. BMAL1 (AUx10'000)
A549
shBMAL1
B
x10^6
shBMAL1
CFU/ml
A549
Hours after synchronisation
C
shBMAL1
Fold Change CFU
A549
Hours after synchronisation
D
CFU/ml x 10^6
A549 shBMAL1
E
CFU/ml x 10^6
A549 shBMAL1
F
Uninfected
Infected
A549
shBMAL1
G
S. aureus / cell
A549
shBMAL1 A549

312

313 **Figure 2. The canonical circadian clock is necessary for rhythm of S. aureus**
314 **invasion, with clock-disrupted cells more permissive for S. aureus invasion. A)**
315 Western blot of parental and *shBMAL1* A549 cell lysates confirms BMAL1 knockdown.
316 Quantitation of band intensities relative to ACTIN showed an approximately 2-fold
317 reduction, N = 3, **P* = 0.0166, unpaired t-test. Time-series of *S. aureus* invasion in
318 parental (black: A549) and *shBMAL1* (red: *shBMAL1*) A549 cells performed as
319 described in Figure 1A showing (**B**) bacterial colony counts (CFU/ml) and (**C**) fold
320 change relative to the unsynchronized control. Dotted lines on graphs show the level
321 of infection of unsynchronized control cells of each cell line. Best fit for COSINOR or
322 linear model show depending on sum-of-squares F-Test as described in Methods
323 section. Unsynchronised parental and *shBMAL1* A549 cells with no synchronization
324 were infected with *S. aureus* JE2 for 1 h, extracellular bacteria removed and cells
325 further incubated for 24 h in the presence of lysostaphin (2 μg/ml). Intracellular
326 bacterial counts after (**D**) 1 h and (**E**) 24 h post infection. N = 3, mean+/-SD, ***P* <
327 0.01, ****P* < 0.001, unpaired t-test. (**F**) Confocal images from infected and uninfected
328 cells 1 h after infection, Red- actin stained by Phalloidin Alexa fluor 647, Blue- bacterial
329 DNA and cell nuclei stained by DAPI. Scale bar = 10 μm. Single Z-sections are shown
330 (**G**) Quantification of intracellular bacteria relative to number of mammalian cells from
331 confocal images from 3 independent experiments, N = 3, *P* = 0.0022, unpaired t-test.

332

333 **Effects of sh*BMAL1* knockdown on the lung epithelial cell transcriptome**

334 To investigate the potential mechanisms underlying the increased bacterial uptake
335 after infection with *S. aureus* 12 h versus 24 h post synchronisation and the time-
336 invariant increase in sh*BMAL1* knockdown cells, we sequenced the transcriptome of
337 parental and sh*BMAL1* lines at 12 h and 24 h post synchronisation. The resulting
338 principal component analysis indicated good separation by cell line (significant
339 correlation with PC1, *P* = 9.75e-07, Figure 3A). First, we considered the differences
340 between the two sequenced cell lines by pooling all samples from the two experimental
341 time points (i.e., 12 and 24 hours after synchronisation). DESeq2 analysis identified a
342 total of 3693 differentially expressed genes (DEGs, 1773 up and 1920 downregulated)
343 in shBMAL1 knockdown vs. parental A549 cells. Furthermore, 29 and three genes
344 were significantly down or up-regulated, respectively, at 12 h compared to 24 h post

345 synchronisation, and no DEGs were found for the interaction term of cell line and
346 timing. Given the low number of samples, this was not unsurprising. However, pathway
347 analysis using PGSEA indicated that 17 KEGG pathways were significantly enriched
348 (Figure 3B). Reassuringly, "circadian rhythms" was significantly less active in the
349 knockdown cells (Figure 3B, Figure S2D). Of the other 16 pathways, at least half have
350 some relevance with infection and inflammation processes. Interestingly, "*S. aureus*
351 infection" was among the pathways significantly enriched (Figure 3B).

352 Contrary to expectations, we did not observe consistent changes in the expression of
353 genes encoding integrins α5 and β1, the receptors to which *S. aureus* adhesins
354 fibronectin binding proteins, Fnbp A and Fnbp B, bind to for the invasion of epithelial
355 cells[31,32]. The gene encoding for *ITGA5* was not significantly changed, and *ITGB1* was
356 even significantly downregulated (Figure 3C). However, when we systematically
357 assessed all integrin isoforms and other extracellular proteins known to be involved in
358 *S. aureus* invasion, we found several other integrin isoforms, e.g., *ITGB2* and *ITGB5*
359 upregulated in the *shBMAL1* A549 cells (Figure 3C).

360

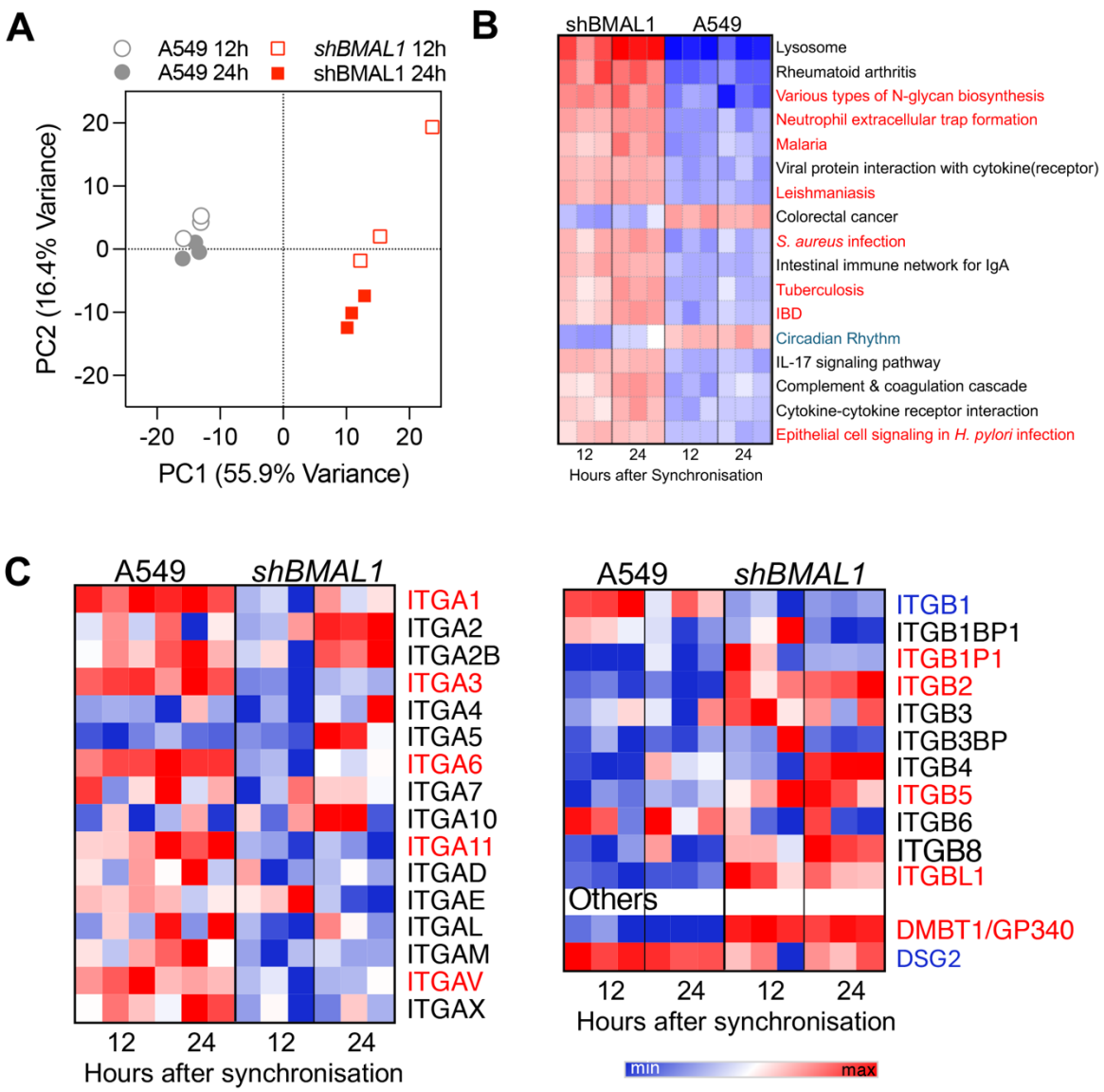

361

362 **Figure 3. *BMAL1* knockdown cells exhibit significant changes in gene**
363 **expression.** (**A**) PCA plot comparing the variance in gene expression by RNA-Seq
364 between parental and shBMAL1 A549 cells collected at 12 h and 24 h after
365 synchronization. (**B**) Significantly regulated KEGG pathways by PGPSEA analysis.
366 Pathways in red font are infection and blue font circadian rhythm related. (**C**)
367 Heatmap showing gene expression profiles for genes encoding integrin A (ITGA)
368 and B (ITGB) subunits and other receptors (DMBT1/GP340) involved in *S. aureus*
369 uptake profiles in parental and *shBMAL1* A549 cells. Names of differentially
370 expressed genes in red font.

371

372 Another differentially expressed gene which was previously recognised to be
373 important for *S. aureus* uptake is GP340[33,34] (Figure 3C). When we compared
374 GP340 coding gene (*DMBT1*) expression at 12 vs. 24 hours after synchronisation,
375 there was only a subtle difference (Figure 4A). In line with our above observations,
376 however, we observed a substantial upregulation of the *GP340* coding gene in
377 *BMAL1* knockdown cells (Figure 4A). We further characterised GP340 protein
378 dynamics using flow cytometry on non-permeabilised live cells and confirmed a 4-
379 fold higher GP340 expression in *shBMAL1* compared to parental A549 cells (Figure
380 4B). Reassuringly a higher abundance of GP340 positive cells at 12 hours after
381 synchronisation compared to 18 and 24 hours after synchronisation (Figure 4 C,D,
382 Kruskal-Wallis, $P = 0.0029$, adj. P of Dunn's post-hoc 12 vs. 18 $P = 0.0033$, 12 vs 24
383 $P = 0.0075$).The COSINOR analysis suggested a rhythmic pattern with 24-hour
384 period was the better fit for the data (COSINOR vs. line: $P = 0.0084$). The bacterial
385 ligand to GP340 is the *S. aureus SraP* protein, which has been reported to facilitate
386 bacterial uptake[33,34]. Thus, *GP340* may be important in the circadian modulation of
387 *S. aureus* uptake.

388

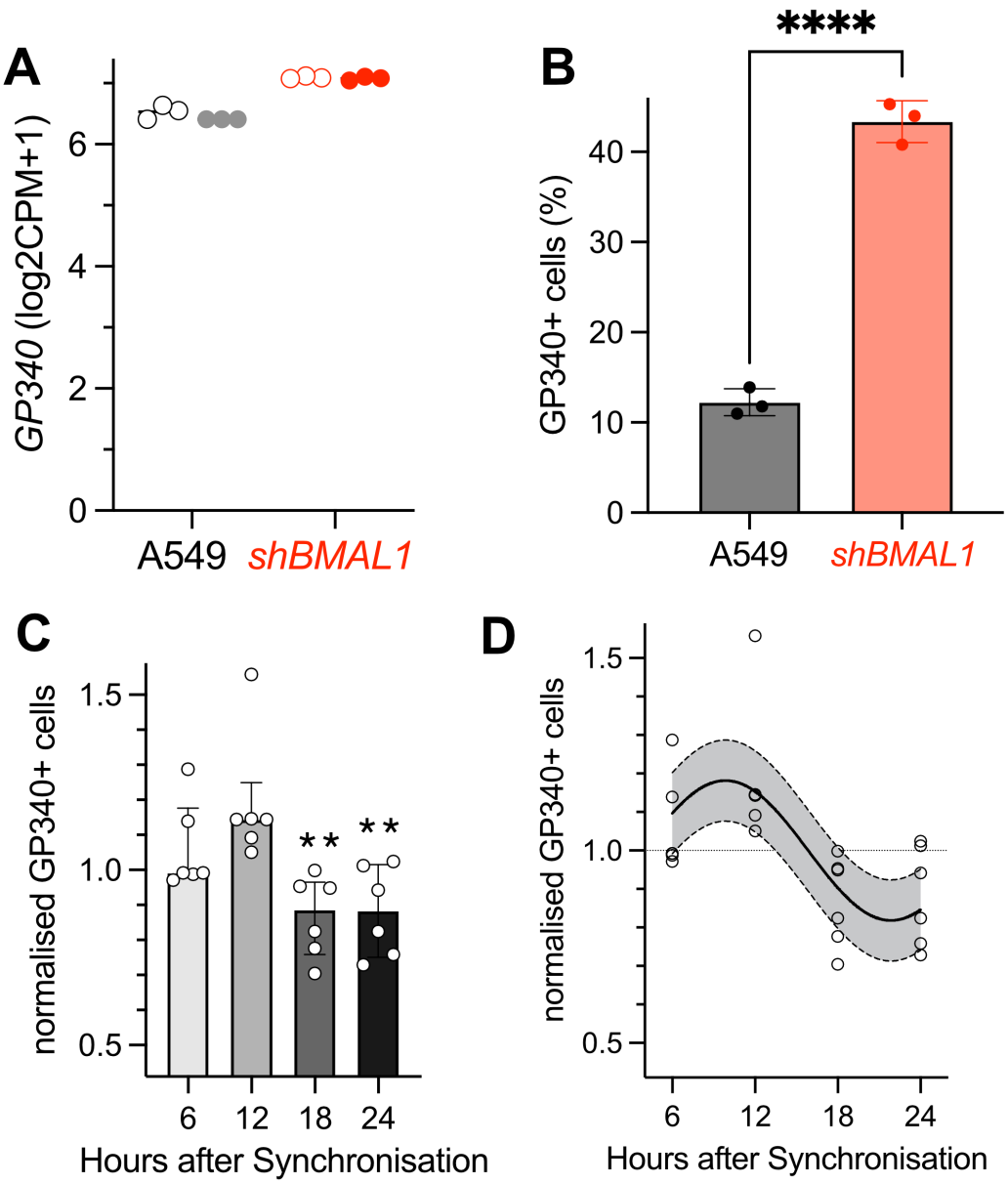

389

390 **Figure 4. GP340 protein expression exhibits a daily rhythm in A549 cells and is**
391 **increase in *BMAL1* knockdown cells.** (**A**) Normalised gene expression of GP340

392 at 12 h (open circles) and 24 h (closed circles) in parental A549 and *shBMAL1*
393 knockdown cells. (**B**) Proportion of GP340 positive cells assessed by flow cytometry
394 is increased (t-test, P <0.0001) in *shBMAL1* compared to A549 parental line. (**C&D**)
395 In A549 cells, GP340 protein expression levels were higher at 12 hours after FSK
396 synchronization compared to 18 and 24 hours (Kruskal-Wallis test, P = 0.0029.
397 Dunn's test: 12 vs. 18: P = 0.0033 and 12 vs. 24: P =0.0075). Expression levels were
398 normalized to median number of GP340+ cells. Model comparison suggested
399 COSINOR to be the preferred fit when compared to linear (P = 0.0084, Best fit for
400 COSINOR or linear model show depending on sum-of-squares F-Test as described
401 in Methods section).

402

403 **The *S. aureus* adhesin *SraP* mediates higher bacterial uptake by *shBMAL1* cells**

404 To directly test the role of *GP340* in rhythmic *S. aureus* invasion, we compared the
405 internalisation of an *S. aureus sraP* mutant with the WT JE2 strain used above in
406 both, the parental and *shBMAL1* A549 cells. Consistent with the data shown in
407 Figures 2 and 3, the uptake of *S. aureus* JE2 by sh*BMAL1* knockdown cells was
408 significantly increased compared to parental A549 cells, however, uptake of the *sraP*
409 mutants in *shBMAL1* was similar to that by the parental A549 cells (Figure 5A).
410 Importantly, in both cell lines, and consistent with Figures 1 and 2, JE2 but not s*raP*
411 mutants showed rhythmic invasion in A549 cells. As expected, both strains did not
412 show rhythmic invasion into *shBMAL1* A549 cells (Figure 5B), but a much higher
413 invasion in non-synchronised cells (Figure 5A).

414 Additionally, we infected both cell types with transposon mutants lacking FnbpA and
415 FnbpB), key *S. aureus* adhesins/invasins. We observed that while the uptake of
416 these mutants was also higher in *shBMAL1* when compared to parental A549 cells,
417 there was no difference when we compared fold changes relative to WT JE2 (Figure
418 S3B). Thus, in contrast to other adhesins tested, our data suggest that *S. aureus*
419 SraP mediate rhythmic bacterial uptake through GP340 and the observed increase
420 in *BMAL1* knockdown cells.

421

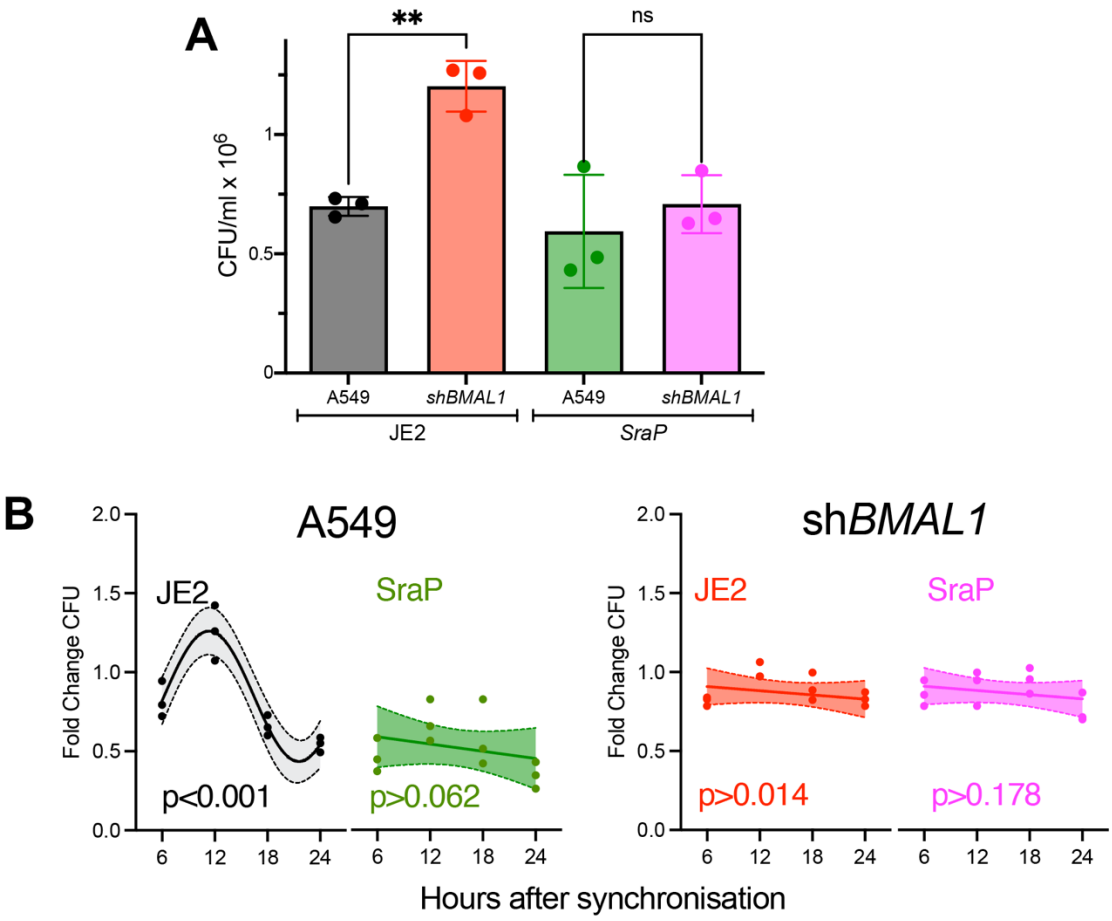

422

423 **Figure 5. GP340 ligand SraP mediates the rhythmic uptake of *S. aureus* in lung**
424 **epithelial cells.** (**A**) Non-synchronized parental and *shBMAL1* A549 cells were
425 infected with WT *S. aureus* (JE2) or *S. aureus sraP* transposon mutant for 1 h, and
426 intracellular bacterial numbers as measured by CFU were compared, ** $P < 0.01$ by
427 an unpaired t-test (**B**) Infection of *S. aureus* JE2 and *sraP* mutant at four times after
428 synchronization of cells with FSK as in Figure 1. The fold changes of CFU for each
429 strain and time compared to the respective control of unsynchronized cells of hat strain
430 are plotted. COSINOR and linear model fit are compared by extra sum of squares F-
431 test and better fit is plotted as described in Methods section. N = 3.

432

433 **Discussion**

434 The ability of *S. aureus* to invade and survive within mammalian cells has been
435 attributed to bacterial persistence, antibiotic resistance and recurrent infections.

436 Although *S. aureus* factors that enable cell invasion have been well studied, the host
437 cellular pathways that mediate this are less understood. Circadian rhythms have been
438 demonstrated to influence several host immune responses during infection with some
439 bacteria exhibiting time-of-day differences in infecting flies and mice[10]. However, at
440 the cellular level, the role of the circadian clock in controlling pathogen invasion or
441 intracellular survival is not known. Here we provide evidence for the role of the
442 mammalian circadian clock in modulating invasion of *Staphylococcus aureus* in human
443 lung epithelial A549 cells. We found significant temporal variations in bacterial uptake,
444 a peak in invasion 12 h after forskolin (FSK) synchronisation of the A549 cells and a
445 marked decrease 24 h post synchronisation. Disrupting the clock through *shBMAL1*
446 knockdown not only abrogated the rhythm in invasion, but also increased the bacterial
447 load, highlighting the influence of the canonical circadian clock in host-pathogen
448 interactions at a cellular level. Notably, using transcriptomic and protein expression
449 analysis, we identified a significant rhythm in GP340 protein abundance and
450 upregulation of *GP340* in the clock-disrupted *shBMAL1* A549 cells. GP340 is known
451 to be a key factor for the uptake of *S. aureus* by epithelial cells through the *S. aureus*
452 adhesin SraP[33-35], and our data suggest that GP340 may mediate the rhythmic uptake
453 of bacteria.

454 Circadian regulation of immune responses is well documented, with evidence
455 suggesting that various immune processes, including cytokine production and
456 phagocytosis, exhibit circadian variations[36]. Colonisation by bacterial pathogens
457 including *Salmonella typhimurium, Streptococcus pneumoniae and S. aureus* have
458 been shown to be impacted by the time of the day, primarily driven by clock-dependent
459 immune responses to infection[37]. As intracellular survival of many of these pathogens
460 have been reported to be an important feature of bacterial pathogenesis, our findings
461 could be relevant for multiple intracellular pathogens. Our findings extend this
462 knowledge by demonstrating that synchronization with FSK not only impacts the
463 invasion of *S. aureus* but also alters the intracellular responses to bacterial challenge.

464 *BMAL1* has a key role in the regulation of circadian rhythms[30]. This complex also
465 activates the transcription of negative regulators, which feedback to inhibit BMAL1-
466 CLOCK activity, ensuring tightly regulated 24-hour rhythms in gene expression[38]. It
467 has been shown that the circadian transcription factor BMAL1 modulates hepatitis C
468 virus (HCV) entry into hepatocytes by regulating the expression of the viral receptors

469 *Cd81* and *Claudin-1*[39]. Pharmacological inhibition of *Bmal1* by REV-ERB agonists
470 reduced *Cd81* and *Claudin-1* expression and inhibited viral entry in cells[39]. Similarly,
471 this was found to down-regulated *angiotensin-converting enzyme 2* expression, which
472 is essential for the entry and replication of SARS-CoV-2 in lung epithelial cells[40]. This
473 highlights the importance of circadian processes for the treatment of viral infection. In
474 addition, various parasitic infections are also linked with regulation of circadian clock[12].
475 Importantly, it has been reported that the complete loss of circadian regulation in
476 *Bmal1* knockout macrophages alters the structure of actin cytoskeleton, which is
477 coupled with a significant increase in *S. pneumoniae* burden compared to WT cells,
478 emphasizing a role for *Bmal1* in limiting bacterial uptake and proliferation[41].

479 Our data demonstrated increased bacterial uptake in *BMAL1* knockdown cells, which
480 occurred independent of the uptake effects of FSK-mediated circadian
481 synchronization of the population. Thus, the temporal modulation in bacterial uptake
482 cannot be explained by the effect of FSK on cAMP induction per se but establishes a
483 role for *BMAL1*-regulated processes in host susceptibility to *S. aureus* invasion. These
484 observations align with the report that BMAL1 deficiency impacts immune cell function
485 and can modulate inflammatory responses[42].

486 Microbial surface components recognizing adhesive matrix molecules (MSCRAMMs)
487 are most prominent surface proteins expressed by staphylococci, which facilitate
488 adhesion to the extracellular matrix (ECM) components such as collagen, fibrinogen,
489 and fibronectin (Fn)[43]. Although, the fibronectin-binding protein (FnBP)–fibronectin
490 (Fn)–α5β1 integrin pathway is the primary route for *S. aureus* internalization[32,44], we
491 did not find upregulation of the main integrins α5β1 in parental vs. *shBMAL1* A549
492 cells. Although *fnbA* and *fnbB* mutants showed reduced uptake in parental cells, they
493 showed higher invasion in *shBMAL1* A549 cells, suggesting involvement of secondary
494 mechanisms in bacterial uptake. We have not used a double mutant lacking both *fnbA*
495 and *fnbB* in this study, so a role of Fnb proteins cannot be fully ruled out. As we
496 observed differential regulation of several integrin isoforms in the RNA-seq results, it
497 is possible that these other isoforms are potentially involved in bacterial uptake. The
498 specific roles of such isoforms in *S. aureus* uptake, however, have not been
499 extensively studied and their potential involvement in bacterial uptake warrants further
500 investigation. As BMAL1 can impact multiple cell signalling pathways, these may also
501 contribute to the increased bacterial uptake[45].

502 Fibronectin-independent mechanisms are known to mediate *S. aureus* entry and
503 involve distinct surface proteins such as serine-aspartate repeat-containing protein D
504 (SdrD), clumping factor A (ClfA), autolysin (Atl), and serine-rich adhesin for platelets
505 (SraP) [43]. SdrD directly binds Desmoglein 1 (encoded by *DSG1*)[46], ClfA interacts with
506 host cells either directly or via fibrinogen bridges[47] and Atl associates with heat shock
507 cognate protein 70 (*HSPA8*)[48], while SraP binds to the salivary scavenger receptor
508 GP340[33,34]. Interestingly, we found a notable rhythm in GP340 protein expression.
509 Circadian disrupted shB*MAL1* knockdown cells, showed increase GP340 gene and
510 protein expression and a reduced invasion of *sraP* mutant strains, suggesting a role
511 for the SraP-GP340 pathway in the circadian modulation of bacterial invasion. SraP,
512 a member of a family of serine rich glycoproteins encoded by Gram positive bacteria
513 including *Streptococcus spp*[35], was shown to mediate adhesion to epithelial cells
514 through its L-lectin binding module[33]. It was also recently reported to modulate
515 macrophage apoptosis and inflammation, indicating its role in *S. aureus*-immune cell
516 interactions[49]. While GP340 is implicated as a receptor in clock-dependent *S. aureus*
517 invasion, it could serve as a co-receptor with other integrins, mediating alternative
518 mechanisms of invasion.

519 Despite the robust findings of this study, our data are from an epithelial cell line (A549)
520 which may limit the generalizability of the results across different cell types and
521 physiological contexts. Future studies should examine the impact of circadian rhythms
522 on *S. aureus* invasion in a broader range of epithelial and immune cell types, in
523 particular immune cells to link these findings better to previous studies on circadian
524 effects in immune responses. Additionally, while our study provides insights into the
525 role of *BMAL1* in regulating bacterial invasion, the specific downstream signalling
526 pathways and molecular mechanisms to understand how circadian rhythms influence
527 the expression of key receptors involved in bacterial invasion remain to be elucidated.

528 The implications of the findings from this study extend to the potential for developing
529 therapeutic strategies that target circadian rhythms to improve the timing and efficacy
530 of antimicrobial treatments. For instance, studies have shown that administering
531 antibiotics in alignment with the host circadian cycle can enhance their effectiveness
532 and reduce side effects[50]. Recent studies have reported intestinal clocks to control the
533 gut microbiota composition and function[51], with enteric bacteria also responding to
534 gastrointestinal hormones like melatonin[52]. While circadian clocks have been only

535 recently described in bacteria[53,54], it would be interesting to study if bacterial
536 pathogens have circadian rhythms and if these pathogen clocks interact with
537 mammalian clocks. Such interacting clocks have been described elsewhere, for
538 example in legumes and rhizobia[55].

539 In conclusion, our study highlights the critical role of circadian rhythms in modulating
540 the dynamics of *S. aureus* invasion in epithelial cells. Overall, our results highlight the
541 critical interplay between circadian biology and microbial pathogenesis, suggesting
542 that manipulation of circadian pathways may provide new avenues for innovative
543 strategies aimed at preventing and treating bacterial infections.

544 **Acknowledgements**

545 We are grateful for funding from the Warwick Research Development Fund (RD and
546 MU) and a Monash Warwick Alliance fellowship to PA (MU). Anglo American Platinum
547 is gratefully acknowledged for funding work in RDs group, and James Jarrold for help
548 with sample collection. Zijin Zhang is thanked for generating the A549 Per2-luc
549 bioluminescence data. We acknowledge use of the flow cytometry equipment and the
550 support provided by the Bio-Analytical Shared Resource Laboratories within the
551 University of Warwick. We thank Vadim Vasilyev for advice on the RNASeq analysis.

552 **Author contributions**

553 P.A. designed and carried out the experimental work, analysed the resulting data
554 and co-wrote the manuscript.

555 G.C., S.N. and J.G. contributed to the experimental design, carried out experimental
556 work and contributed to data analysis and writing of the manuscript.

557 R.D. and M.U. jointly supervised the work, and contributed to formal analysis, writing
558 of the manuscript and acquisition of funding.

Competing interests

The authors declare no competing interests.

561 **Data availability**

562 Summary data are depicted in the figures. Raw data are available from the
563 corresponding authors upon reasonable request. RNA-Seq data are available at the
564 ELIXIR database ArrayExpress under accession number E-MTAB-15036.

565 **References**

566 1 Takahashi, J. S. Transcriptional architecture of the mammalian circadian clock.
567 *Nature Reviews Genetics* **18**, 164-179 (2017).
568 2 Wollmuth, E. M. & Angert, E. R. Microbial circadian clocks: host-microbe
569 interplay in diel cycles. *BMC microbiology* **23**, 124 (2023).
570 3 Bass, J. & Takahashi, J. S. Circadian integration of metabolism and energetics.
571 *Science* **330**, 1349-1354 (2010). https://doi.org:10.1126/science.1195027
572 4 Scheiermann, C., Gibbs, J., Ince, L. & Loudon, A. Clocking in to immunity. *Nat*
573 *Rev Immunol* **18**, 423-437 (2018). https://doi.org:10.1038/s41577-018-0008-4
574 5 Shim, D. W. *et al.* Deficiency of circadian clock gene Bmal1 exacerbates
575 noncanonical inflammasome-mediated pyroptosis and lethality via Rev-erbα-
576 C/EBPβ-SAA1 axis. *Experimental and Molecular Medicine* **56**, 370-382 (2024).
577 https://doi.org:10.1038/s12276-024-01162-w
578 6 Haspel, J. A. *et al.* Perfect timing: circadian rhythms, sleep, and immunity - an
579 NIH workshop summary. *JCI Insight* **5**, e131487,-131487 (2020).
580 https://doi.org:10.1172/jci.insight.131487
581 7 Scheiermann, C., Kunisaki, Y. & Frenette, P. S. Circadian control of the immune
582 system. *Nat Rev Immunol* **13**, 190-198 (2013). https://doi.org:10.1038/nri3386
583 8 Jerigova, V., Zeman, M. & Okuliarova, M. Circadian Disruption and
584 Consequences on Innate Immunity and Inflammatory Response. *Int J Mol Sci*
585 **23** (2022). https://doi.org:10.3390/ijms232213722
586 9 Curtis, A. M., Bellet, M. M., Sassone-Corsi, P. & O'Neill, L. A. Circadian clock
587 proteins and immunity. *Immunity* **40**, 178-186 (2014).
588 https://doi.org:10.1016/j.immuni.2014.02.002
589 10 Rijo-Ferreira, F. & Takahashi, J. S. Circadian rhythms in infectious diseases
590 and symbiosis. *Semin Cell Dev Biol* **126**, 37-44 (2022).
591 https://doi.org:10.1016/j.semcdb.2021.09.004
592 11 Lowy, F. D. Staphylococcus aureus Infections. *New England Journal of*
593 *Medicine* **339**, 520-532 (1998).
594 https://doi.org:10.1056/NEJM199808203390806
595 12 David, M. Z. & Daum, R. S. Community-associated methicillin-resistant
596 Staphylococcus aureus: epidemiology and clinical consequences of an

597 emerging epidemic. *Clin Microbiol Rev* **23**, 616-687 (2010).
598 https://doi.org:10.1128/CMR.00081-09
599 13 Moldovan, A. & Fraunholz, M. J. In or out: Phagosomal escape of
600 Staphylococcus aureus. *Cell Microbiol* **21**, e12997 (2019).
601 https://doi.org:10.1111/cmi.12997
602 14 Watkins, K. E. & Unnikrishnan, M. Evasion of host defenses by intracellular
603 Staphylococcus aureus. *Adv Appl Microbiol* **112**, 105-141 (2020).
604 https://doi.org:10.1016/bs.aambs.2020.05.001
605 15 Marro, F. C. *et al.* In vitro antibiotic activity against intraosteoblastic
606 Staphylococcus aureus: a narrative review of the literature. *J Antimicrob*
607 *Chemother* **76**, 3091-3102 (2021). https://doi.org:10.1093/jac/dkab301
608 16 Peyrusson, F. *et al.* Intracellular Staphylococcus aureus persisters upon
609 antibiotic exposure. *Nat Commun* **11**, 2200 (2020).
610 https://doi.org:10.1038/s41467-020-15966-7
611 17 Tsujihana, K. *et al.* Circadian protection against bacterial skin infection by
612 epidermal CXCL14-mediated innate immunity. *Proc Natl Acad Sci U S A* **119**,
613 e2116027119 (2022). https://doi.org:10.1073/pnas.2116027119
614 18 Balsalobre, A., Marcacci, L. & Schibler, U. Multiple signaling pathways elicit
615 circadian gene expression in cultured Rat-1 fibroblasts. *Curr Biol* **10**, 1291-1294
616 (2000). https://doi.org:10.1016/s0960-9822(00)00758-2
617 19 Yagita, K. & Okamura, H. Forskolin induces circadian gene expression of rPer1,
618 rPer2 and dbp in mammalian rat-1 fibroblasts. *FEBS Lett* **465**, 79-82 (2000).
619 https://doi.org:10.1016/s0014-5793(99)01724-x
620 20 Maier, B., Lorenzen, S., Finger, A. M., Herzel, H. & Kramer, A. Searching Novel
621 Clock Genes Using RNAi-Based Screening. *Methods Mol Biol* **2130**, 103-114
622 (2021). https://doi.org:10.1007/978-1-0716-0381-9_8
623 21 Zhang, Y. *et al.* Dosing time dependent in vitro pharmacodynamics of
624 Everolimus despite a defective circadian clock. *Cell Cycle* **17**, 33-42 (2018).
625 https://doi.org:10.1080/15384101.2017.1387695
626 22 Mastrullo, V. *et al.* Pericytes' Circadian Clock Affects Endothelial Cells'
627 Synchronization and Angiogenesis in a 3D Tissue Engineered Scaffold. *Front*
628 *Pharmacol* **13**, 867070 (2022). https://doi.org:10.3389/fphar.2022.867070

629 23 Torre, D., Lachmann, A. & Ma'ayan, A. BioJupies: Automated Generation of
630 Interactive Notebooks for RNA-Seq Data Analysis in the Cloud. *Cell Syst* **7**,
631 556-561 e553 (2018). https://doi.org:10.1016/j.cels.2018.10.007
632 24 Ge, S. X., Son, E. W. & Yao, R. iDEP: an integrated web application for
633 differential expression and pathway analysis of RNA-Seq data. *BMC*
634 *Bioinformatics* **19**, 534 (2018). https://doi.org:10.1186/s12859-018-2486-6
635 25 Anders, S. & Huber, W. Differential expression analysis for sequence count
636 data. *Genome Biol* **11**, R106 (2010). https://doi.org:10.1186/gb-2010-11-10-
637 r106
638 26 Robinson, M. D., McCarthy, D. J. & Smyth, G. K. edgeR: a Bioconductor
639 package for differential expression analysis of digital gene expression data.
640 *Bioinformatics* **26**, 139-140 (2010).
641 https://doi.org:10.1093/bioinformatics/btp616
642 27 Kim, S. Y. & Volsky, D. J. PAGE: parametric analysis of gene set enrichment.
643 *BMC Bioinformatics* **6**, 144 (2005). https://doi.org:10.1186/1471-2105-6-144
644 28 Schindelin, J. *et al.* Fiji: an open-source platform for biological-image analysis.
645 *Nat Methods* **9**, 676-682 (2012). https://doi.org:10.1038/nmeth.2019
646 29 Fang, G., Chen, Q., Li, J., Lian, X. & Shi, D. The Diurnal Transcriptome Reveals
647 the Reprogramming of Lung Adenocarcinoma Cells Under a Time-Restricted
648 Feeding-Mimicking Regimen. *J Nutr* **154**, 354-368 (2024).
649 https://doi.org:10.1016/j.tjnut.2023.11.033
650 30 Bunger, M. K. *et al.* Mop3 is an essential component of the master circadian
651 pacemaker in mammals. *Cell* **103**, 1009-1017 (2000).
652 https://doi.org:10.1016/s0092-8674(00)00205-1
653 31 Niemann, S. *et al.* Correction for Niemann et al., "More Is Not Always Better-
654 the Double-Headed Role of Fibronectin in Staphylococcus aureus Host Cell
655 Invasion". *mBio* **14**, e0292123 (2023). https://doi.org:10.1128/mbio.02921-23
656 32 Sinha, B. *et al.* Fibronectin-binding protein acts as Staphylococcus aureus
657 invasin via fibronectin bridging to integrin alpha5beta1. *Cell Microbiol* **1**, 101-
658 117 (1999). https://doi.org:10.1046/j.1462-5822.1999.00011.x
659 33 Zhou, T.-T. *et al.* Monoclonal antibody against I-lectin module of SraP blocks
660 adhesion and protects mice against Staphylococcus aureus challenge.
661 *Journal of Microbiology, Immunology and Infection* **54**, 420-428 (2021).
662 https://doi.org:10.1016/j.jmii.2019.08.019

663 34 Kukita, K. *et al.* Staphylococcus aureus SasA is responsible for binding to the
664 salivary agglutinin gp340, derived from human saliva. *Infection and Immunity*
665 **81**, 1870-1879 (2013). https://doi.org:10.1128/IAI.00011-13
666 35 Yang, Y. H. *et al.* Structural insights into SraP-mediated Staphylococcus aureus
667 adhesion to host cells. *PLoS Pathog* **10**, e1004169 (2014).
668 https://doi.org:10.1371/journal.ppat.1004169
669 36 Arjona, A. & Sarkar, D. K. Are circadian rhythms the code of hypothalamic-
670 immune communication? Insights from natural killer cells. *Neurochem Res* **33**,
671 708-718 (2008). https://doi.org:10.1007/s11064-007-9501-z
672 37 Tognini, P., Thaiss, C. A., Elinav, E. & Sassone-Corsi, P. Circadian
673 Coordination of Antimicrobial Responses. *Cell Host Microbe* **22**, 185-192
674 (2017). https://doi.org:10.1016/j.chom.2017.07.007
675 38 Abe, Y. O. *et al.* Rhythmic transcription of Bmal1 stabilizes the circadian
676 timekeeping system in mammals. *Nature Communications* **13**, 4652 (2022).
677 https://doi.org:10.1038/s41467-022-32326-9
678 39 Zhuang, X. *et al.* The circadian clock components BMAL1 and REV-ERBα
679 regulate flavivirus replication. *Nature Communications* **10** (2019).
680 https://doi.org:10.1038/s41467-019-08299-7
681 40 Zhuang, X. *et al.* The circadian clock component BMAL1 regulates SARS-CoV-
682 2 entry and replication in lung epithelial cells. *iScience* **24**, 103144 (2021).
683 https://doi.org:10.1016/j.isci.2021.103144
684 41 Kitchen, G. B. *et al.* The clock gene Bmal1 inhibits macrophage motility,
685 phagocytosis, and impairs defense against pneumonia. *Proc Natl Acad Sci U*
686 *S A* **117**, 1543-1551 (2020). https://doi.org:10.1073/pnas.1915932117
687 42 Keller, M. *et al.* A circadian clock in macrophages controls inflammatory
688 immune responses. *Proc Natl Acad Sci U S A* **106**, 21407-21412 (2009).
689 https://doi.org:10.1073/pnas.0906361106
690 43 Josse, J., Laurent, F. & Diot, A. Staphylococcal Adhesion and Host Cell
691 Invasion: Fibronectin-Binding and Other Mechanisms. *Front Microbiol* **8**, 2433
692 (2017). https://doi.org:10.3389/fmicb.2017.02433
693 44 Massey, R. C. *et al.* Fibronectin-binding protein A of Staphylococcus aureus
694 has multiple, substituting, binding regions that mediate adherence to fibronectin
695 and invasion of endothelial cells. *Cell Microbiol* **3**, 839-851 (2001).
696 https://doi.org:10.1046/j.1462-5822.2001.00157.x

697 45 Jung, C. H. *et al.* Bmal1 suppresses cancer cell invasion by blocking the
698 phosphoinositide 3-kinase-Akt-MMP-2 signaling pathway. *Oncol Rep* **29**, 2109-
699 2113 (2013). https://doi.org:10.3892/or.2013.2381
700 46 Askarian, F. *et al.* The interaction between Staphylococcus aureus SdrD and
701 desmoglein 1 is important for adhesion to host cells. *Sci Rep* **6**, 22134 (2016).
702 https://doi.org:10.1038/srep22134
703 47 Geoghegan, J. A. *et al.* Molecular characterization of the interaction of
704 staphylococcal microbial surface components recognizing adhesive matrix
705 molecules (MSCRAMM) ClfA and Fbl with fibrinogen. *J Biol Chem* **285**, 6208-
706 6216 (2010). https://doi.org:10.1074/jbc.M109.062208
707 48 Hirschhausen, N. *et al.* A novel staphylococcal internalization mechanism
708 involves the major autolysin Atl and heat shock cognate protein Hsc70 as host
709 cell receptor. *Cell Microbiol* **12**, 1746-1764 (2010).
710 https://doi.org:10.1111/j.1462-5822.2010.01506.x
711 49 Sun, H., Li, R. W., Wang, T. T. Y. & Ding, L. The Ligand Binding Domain of the
712 Cell Wall Protein SraP Modulates Macrophage Apoptosis and Inflammatory
713 Responses in Staphylococcus aureus Infections. *Molecules* **30** (2025).
714 https://doi.org:10.3390/molecules30051168
715 50 Lee, Y., Field, J. M. & Sehgal, A. Circadian Rhythms, Disease and
716 Chronotherapy. *J Biol Rhythms* **36**, 503-531 (2021).
717 https://doi.org:10.1177/07487304211044301
718 51 Heddes, M. *et al.* The intestinal clock drives the microbiome to maintain
719 gastrointestinal homeostasis. *Nat Commun* **13**, 6068 (2022).
720 https://doi.org:10.1038/s41467-022-33609-x
721 52 Paulose, J. K. & Cassone, V. M. The melatonin-sensitive circadian clock of the
722 enteric bacterium Enterobacter aerogenes. *Gut Microbes* **7**, 424-427 (2016).
723 https://doi.org:10.1080/19490976.2016.1208892
724 53 Eelderink-Chen, Z. *et al.* A circadian clock in a nonphotosynthetic prokaryote.
725 *Sci Adv* **7** (2021). https://doi.org:10.1126/sciadv.abe2086
726 54 Chou, K. T. *et al.* A segmentation clock patterns cellular differentiation in a
727 bacterial biofilm. *Cell* **185**, 145-157 e113 (2022).
728 https://doi.org:10.1016/j.cell.2021.12.001

729 55 Rowson, M., Jolly, M., Dickson, S., Gifford, M. L. & Carre, I. Timely symbiosis:
730 circadian control of legume-rhizobia symbiosis. *Biochem Soc Trans* **52**, 1419-
731 1430 (2024). https://doi.org:10.1042/BST20231307

732